Journal of Natural Fibers

ISSN: 1544-0478 (Print) 1544-046X (Online) Journal homepage: https://www.tandfonline.com/loi/wjnf20

Transition characteristics of Brazilian vegetable fibers investigated by heating microscopy

Beatriz da Silva Machado, Valdinei Sales Martins, Luciano Pisanu & Marcio Luis Ferreira Nascimento

To cite this article: Beatriz da Silva Machado, Valdinei Sales Martins, Luciano Pisanu & Marcio Luis Ferreira Nascimento (2020) Transition characteristics of Brazilian vegetable fibers investigated by heating microscopy, Journal of Natural Fibers, 17:3, 450-462, DOI: 10.1080/15440478.2018.1500337

To link to this article: https://doi.org/10.1080/15440478.2018.1500337

Published online: 01 Aug 2018.

JOURNAL OF NATURAL FIBERS
2020, VOL. 17, NO. 3, 450–462
https://doi.org/10.1080/15440478.2018.1500337

Taylor & Francis
Taylor & Francis Group

Transition characteristics of Brazilian vegetable fibers investigated by heating microscopy

Beatriz da Silva Machado[a], Valdinei Sales Martins[a], Luciano Pisanu [b], and Marcio Luis Ferreira Nascimento [a,c]

[a]PROTEC/PEI - Graduate Program in Industrial Engineering, Department of Chemical Engineering, Polytechnic School, Federal University of Bahia, Salvador, Brazil; [b]SENAI/Cimatec, Salvador, Brazil; [c]Vitreous Materials Lab, Department of Chemical Engineering, Polytechnic School, Federal University of Bahia, Salvador, Brazil

ABSTRACT

Structural studies of three vegetable fibers plus eucalypt wood through heating microscopy, Fourier transform infrared spectroscopy, X-ray diffraction (XRD), and thermal analysis through Thermal Gravimetric Analysis/Differential Thermal Analysis are presented in this work. Morphological and dimensional changes obtained from heating microscopy were observed, showing shrinkage occurrences of vegetable fibers related to their diameter and length, respectively. The thickness decreased by 50% when heated at 450–500°C, this process starting at 300–400°C with an initial percentage length of ≈ 90%, that corresponds to a fast weight loss. These results were compared with simultaneous thermal analysis under the same conditions. Thus, for the first time, it was possible to quantify vegetable fiber dimensional changes and surface aspects under heating that cannot be seen by traditional thermal analysis. We also performed crystallinity calculations from XRD data, observing that cellulose/hemicellulose contents had major contribution in all samples.

摘要

本文通过热显微镜、FTIR、XRD和TGA/DTA热分析对三种植物纤维加桉木的结构进行了研究。观察到加热显微镜下的形态和尺寸变化，表明植物纤维的收缩率与直径和长度有关。在450～500℃加热时，厚度降低了50%，该过程起始于300～400℃，初始百分比为≈90%，相当于快速减肥。在相同条件下，将这些结果与同时热分析进行了比较。因此，第一次有可能量化蔬菜纤维的尺寸变化和表面方面的加热，不能看到传统的热分析。我们还进行了X-射线衍射数据的结晶度计算，观察到纤维素/半纤维素含量在所有样品中都有重要贡献。

KEYWORDS

Vegetable fiber; coconut; sugarcane bagasse; sisal; heating microscopy; crystallinity

关键词

植物纤维; 椰子; 甘蔗甘蔗渣; 剑麻; 加热显微镜; 结晶度。

Introduction

Many studies have evaluated the feasibility of using vegetable fibers as an alternative to synthetic fibers conventionally used as reinforcement in composite polymer matrix materials (Brahmakumar et al. 2005; Sanchez et al. 2010). This interest is due to the need to find renewable raw materials sources with the main objective to reduce the environmental impact for production of new materials with reduced costs. Cellulosic fibers such as sugarcane bagasse, sisal, banana, coconut, and wood have been incorporated in various thermoplastics and thermosets as reinforcement or load due to be important agro-industrial residues (Morandim-Giannetti et al. 2012; Sanchez et al. 2010).

CONTACT Marcio Luis Ferreira Nascimento mlfn@ufba.br PROTEC/PEI - Graduate Program in Industrial Engineering, Department of Chemical Engineering, Polytechnic School, Federal University of Bahia, Rua Aristides Novis 2, Federação, Salvador, BA 40210–630, Brazil

Color versions of one or more of the figures in the article can be found online at www.tandfonline.com/wjnf.

In fact, vegetable fibers are promising materials for the production of biodegradable plastic composites, due to its natural abundance and sustainability, in addition to be capable of exhibit interesting thermoplastic behavior under shear stress as well as interesting applications in higher temperatures when compared with simple polymers (Brigida et al. 2010). However, one of the main drawbacks seems to be the limited thermal stability of such fibers, because its first degradation occurs at temperatures near 200°C, as shown in this work. Other important barrier is due that, in general, vegetable fibers are extremely hydrophilic, which results in a weak interaction with the thermoplastic matrix, which is normally hydrophobic (Brahmakumar *et al.* 2005).

Only after the invention of the optical microscope around the seventeenth century, it was possible to start disclosing the wood fine structure (Kisser et al. 1967), gaining insight into their structure and functions. Cellulose is the main structural component of plant fibers. Its crystalline structure was first established by the Swiss botanists Carl Wilhelm von Nägeli (1817–1891, Figure 1*a*) and Carl Eduard Cramer (1831–1901) in 1858 (Kisser et al. 1967; Nägeli and Cramer 1858). The components lignin and hemicellulose also have an important role in many characteristic properties of such fibers (Sanchez et al. 2010). Hemicellulose is a complex and low molecular weight polysaccharide which includes polymeric carbohydrates having five to six carbon atoms in the structure of their sugar units. The structural complexity of hemicellulose is responsible for properties such as absence of crystallinity, low molar mass, and high water absorption (Sanchez et al. 2010). The tenacity, property of fibers to absorb energy until breaking, is reduced by decreasing the amount of lignin and hemicellulose, while the force increases to a limit value. The removal of lignin in the vegetable fibers allows the production of more rigid fibers (Mwaikambo and Ansell 2006).

Fibers generally have good tensile strength, high modulus of elasticity, high humidity, and good degradability (Brahmakumar et al. 2005; Morandim-Giannetti et al. 2012; Sanchez et al. 2010), but a full comprehension of their properties based on microscopy structure is far from complete. Structural studies through heating microscopy, X-ray diffraction (XRD), Fourier transform infrared

Figure 1. (*a*) Carl Wilhelm von Nägeli (1817–1891), Swiss botanist. (*b*) Salomon Stricker (1834–1898), Austrian pathologist and histologist.

spectroscopy (FTIR), and thermal stability through Thermal Gravimetric Analysis (TGA)/ Differential Thermal Analysis (DTA) are presented in this paper. These analyses have as main objectives first to observe the composition of the fibers, making comparisons between the species studied and analyzing their behavior in different temperatures. In special, we show the behavior of vegetable fibers under heating, comparing images from heating microscopy with TGA/DTA under same conditions.

According to Schmidt (1959), the use of heating microscopy dates back to the nineteenth century and is related to biology applications. There were equipments that used some different principles, as for example: (i) electricity; (ii) conduction through metal plates; (iii) water; (iv) hot air. An electrical setup was recommended by the Austrian pathologist and histologist Salomon Stricker (1834–1898, Figure 1*b*; Stricker 1870). This work presents transition temperature characteristics by means of heating microscopy technique over three different fibers plus a wood powder. Such studies would improve new researches on slow pyrolysis, i.e., the heating of wood or other substances in the absence of oxygen producing wood charcoal (Assis et al. 2016).

Materials and methods

Three Brazilian fibers were analyzed: *sugarcane* from the interior of state of São Paulo; *coconut fiber* from Conde, a municipality in the state of Bahia, supplied by the Frisk Industry (the Aurantiaca Group: www.aurantiaca.com.br); *sisal*, from Coité, another municipality of Bahia; we also analyzed an *eucalyptus* powder, from a reforested wood provided by Venturoli Company (www.venturoli.com.br), from Camaçari municipality, Bahia. They are some of the most important commercial varieties of Brazilian fibers (Brigida et al. 2010).

All analysis was done with untreated vegetable fibers as well as wood powder. Initially, the fibers were hand scraped with the aid of a blade and passed through nylon monofilament sieves below 250 μm. After this first stage, we observed single materials by means of a heating microscopy stage Linkam TS1500 (Tadworth, UK) coupled to a Leica DM 4000 (Wetzlar, Germany) optical microscope using a 50× objective lens, from 300 K to near 800 K at 10 K/min, using platinum pans, observing single fibers and particles (in the case of the eucalypt wood powder). A set of at least 200 fibers of each vegetable type was tested to get meaningful results for length and size, looking for good statistics. Leica DM 4000 M and Image J *softwares* (Bethesda, USA) were employed to analyze the fiber images. Sample position for optical registration device was chosen and fixed to obtain clear focused images.

Thermogravimetric analysis (TGA – Thermogravimetry/DTA – Differential Thermal Analysis), were conducted to evaluate the thermal stability of the fibers. Data were obtained using a DTG Shimadzu 60H (Kyoto, JP). We analyzed the same materials under nitrogen and air atmospheres, with a flow rate of 50 mL/min. These experiments were carried out in a temperature interval of 300–1073 K at 10 K/min, with platinum (Pt) pans and mass samples between 2.8 and 4.2 mg (under N_2) and 0.5 and 1.2 mg (under air), measured using a Mettler-Toledo XS 205 (Columbus, USA) dual range balance. As a reference, a void Pt pan was used for each measurement. The weight loss and its derivative (DTG) as a function of temperature were analyzed.

FTIR Spectroscopy was carried out to qualitatively identify the main constituents of vegetable fibers plus wood powder. FTIR analysis was performed using ground fine materials by means of a Spectrum Two Perkin Elmer Spectrometer (Waltham, USA) with universal Attenuated Total Reflectance (ATR) probe. To obtain FTIR spectra, 10 scans were collected for wave number, ranging from 4000 to 500 cm^{-1}, with resolution of 4 cm^{-1}

Finally, XRD diffraction measurements were conducted in a X-ray diffractometer Shimadzu XRD-6000 (Kyoto, JP), with radiation CuK_α (λ = 1542 Å), 30 kV tension, 15 mA electric current, with 2θ fluctuating of 2–65° and sweep speed of 0.25° per step, with a counting time of 1 s per step. Data were collected using a 0.5 mm divergence slit along with a 0.5 and 0.3 mm receiving slits. Powder fiber samples were placed on an aluminum sample holder, pressed to obtain a regular surface, and inserted in

the diffractometer goniometer support. A silicon standard was used to calibrate the equipment. The qualitative interpretation was performed by comparison with existing standards on PDF-4 database (the International Centre for Diffraction Data, ICDD: www.icdd.com, 2003) using specific software.

The determination of amorphous content in crystalline materials is a key issue for diffractionists (Madsen, Scarlett, and Kern 2011). It is also important to fibers, and many authors cited the problem of cellulose crystallinity index (CI) (Park et al. 2010), that varies significantly depending on the choice of measurement method: XRD, infrared (IR), Raman spectroscopy, and solid-state ^{13}C nuclear magnetic resonance.

Since the work of Segal et al. (1962), the CI is generally calculated from the height ratio between the intensity of the crystalline peak (I_{002}–I_{AM}) and total intensity (I_{002}) after subtraction of the background signal measured without cellulose. Briefly, I_{AM} is the height of the minimum position between the (002) and the (101) peaks, around 18.3° (considering 2θ angle). This technique is named as the *peak height method*.

As the peaks in the cellulose diffraction spectrum are very broad and vary considerably in their width, a simple height comparison is difficult to provide a reasonable estimate of cellulose crystallinity. In fact, Segal et al. (1962) only intended this method to be used as a "time-saving empirical measure of relative crystallinity."

To help on such analysis, according to Madsen, Scarlett, and Kern (2011), one of the easiest ways to quantify amorphous phase or the Degree of Crystallinity (DOC), that is equivalent to CI and follows Equation (1):

$$\mathrm{DOC} = \frac{\text{Crystalline Area}}{\text{Crystalline Area} + \text{Amorphous Area}} \tag{1}$$

This equation is Rietveld-based (Rietveld 1969), i.e., it relies on the estimation of the total intensity or area contributed to the overall pattern by each component in the analysis considering XRD results. Thus, DOC is calculated from the total areas under the defined crystalline and amorphous components. Madsen, Scarlett, and Kern (2011) affirmed that the crystalline area comprises the sum of all area for phases that are not flagged as amorphous while the amorphous area is the converse.

Results and discussion

Brazilian plants generally have a lignin content of 26–34% (Carvalho 2004). Lignin provides stiffness to the cell wall, resulting in good mechanical properties. Wood is classified according to the lignin content. Some woods are considered hard when the lignin content is between 16% and 24% and this classification will determine their applications (Carvalho 2004).

According to Foelkel's classification (1977), celluloses are substances that constitute large polysaccharides chains, and it is in the range of 40–45% of every wood; hemicelluloses are substances that form a matrix involving cellulose, present in the order of 20–30% of every wood; and lignins are fouling substances which fill the voids in the cell wall that constitute about 18–25% and 25–35% of wood in hardwoods and conifers, respectively. The insoluble lignin content showed to be within the range for conifers, with an average of 28% for the material analyzed. According to Sansigolo (1994), wood contains about 15–30% of lignin, the values usually found to be 25–30% and 68.80% of holocellulose (i.e., cellulose plus hemicellulose) for coniferous woods.

Compared with other fibers, sugarcane has lower tensile strength, lower modulus of elasticity, higher moisture content and better degradability due to its high content of hemicellulose. According Satyanaryana, Guimarães, and Wypych (2007), sugarcane has 54.3–55.2% of cellulose, 16.8–29.7% of hemicellulose, and 24–25% of lignin, and the variation of the chemical composition of coconut fiber is between 43.4% and 53% of cellulose, 14.7% hemicellulose, and 38–40% lignin.

The study to determine the chemical composition of the sisal fiber performed by Medina (1954) showed that the fiber consists of 65.8% cellulose, 12% hemicellulose, and 9.9% lignin. These literature values are resumed in Table 1.

Morphological analysis

The first aspect analyzed was the fiber morphology by optical microscopy at room temperature. The results of diameter and average length determination for vegetable fibers are shown at Table 2. The average coconut fiber diameter of 135.8 ± 0.5 μm is in the range observed by Satyanaryana, Guimarães, and Wypych (2007).

A natural dispersion of diameter values was observed for all materials studied in this work due to hand scraper procedure. A greater deviation was observed in relation to length. However, all materials presented monomodal distribution considering length and diameter.

Fourier Transform Infrared (FTIR) spectroscopy

The FTIR spectra of the materials analyzed are shown in Figure 2. In general, all sample spectra presented same band patterns. IR spectra of such fibers indicate which functional groups exist in their composition; each spectra band is related to a group, and they are also related between due to their nature. For example, all these spectra reveal a broad and intense peak at 3340 cm^{-1} due to hydrogen-bonded OH^- stretching vibration from the cellulose and lignin structure of the fiber (Brigida et al. 2010).

The absorptions are related to the axial deformations of the functional component groups (Lopes and Fascio 2004). In this experiment, no KBr was necessary to add to our samples due to universal ATR technique.

The fibers present in their composition are mainly lignin, hemicellulose, and cellulose, as expected. These components are composed of alkenes and aromatic groups, as well as different functional groups containing oxygen, such as esters, ketones, and alcohol. The most intense band attributed to OH^- and CO–C is found for cellulose, while hemicellulose has strong CO^- bands. Evaluating the components individually, the great difference is found in the region of (1830–730 cm^{-1}). The 1100 cm^{-1} vibration bands of C–O–C and C–OH^- at 1060–1050 cm^{-1} refer to the cellulose chain resulting from polysaccharide components. Other peaks due to the alcohol group of the cellulose appear at 1360 and 1320 cm^{-1} (Sgriccia, Hawley, and Misra 2008; Yang et al. 2007). Differences in peak intensity can be also related to the DOC (or the cellulose CI, see Park et al. 2010).

Table 1. Usual lignin, cellulose, and hemicellulose contents of some vegetable fibers found in literature plus DOC percentage from this work.

	Lignin	Cellulose	Hemicellulose	Reference	DOC
Coconut	38–40	43–53	~15	Satyanaryana, Guimarães, and Wypych (2007)	13.9%
Sugarcane	~34	~48	~9	Satyanaryana, Guimarães, and Wypych (2007)	14.9%
Sisal	~10	~66	~12	Medina (1954)	11.1%
Wood	15–30	40–45	20–30	Sansigolo (1994)	16.1%

Table 2. Average length and diameter of the vegetable fibers and wood powder by optical microscopy (50× lens objective) at room temperature observed in this work.

Vegetable Fibers/Wood	Average Length (±0.5 μm)	Average Diameter(±0.5 μm)
Sugar cane bagasse	689.2	201.7
Coconut fiber	1446.3	135.8
Sisal	832.3	172.5
Wood powder	577.1	189.7

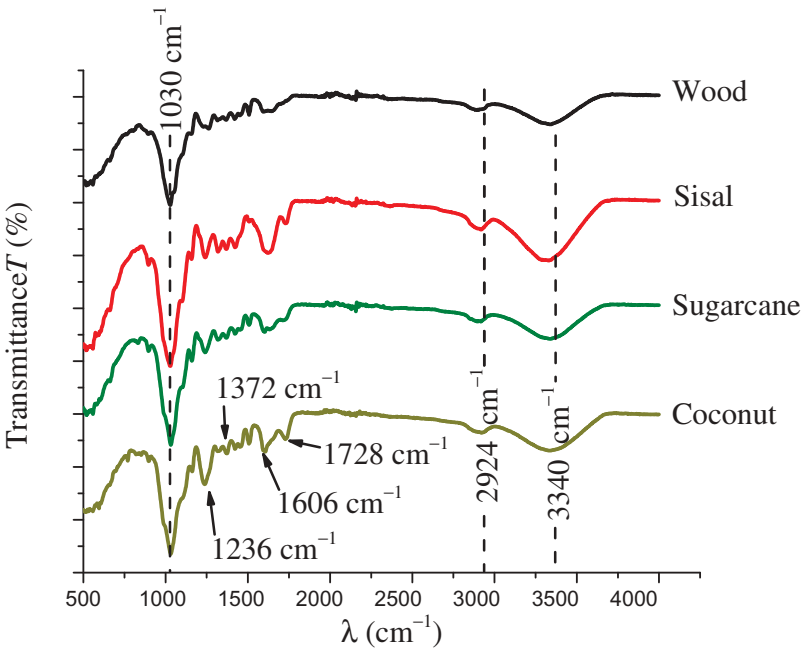

Figure 2. FTIR spectra of three vegetable fibers (coconut, sugarcane, and sisal) plus eucalypt powder. Some vibrational bands are indicated in agreement with literature data.

X-ray diffractometry

Another analysis performed was by means of X-ray diffractometry, and the main objective was to determine more precisely the structure of the natural materials. However, as already mentioned, samples have cellulose and lignin as some of the components that make them partially amorphous. Thus, it verifies the absence of pure crystallinity. X-ray analyses of the materials are shown in Figure 3.

These results are similar to those reported in the literature for other vegetable fibers, which mainly exhibit a cellulosic structure. Experimental results presented peaks related to the characteristic crystal planes of lignocellulosic materials around 22°, corresponding to the coordinate plane of reflection (002), in agreement with ICDD 50–2241 card (cellulose I_β). Second and third small peaks observable at 16° and 35° are related to amorphous portion in microfibriles, i.e., hemicellulose and lignin. One of the first works on the crystalline determination by means of X-rays was done by Herzog and Jancke (1920).

McGinnes, Kandeel, and Szopa (1971) compared XRD patterns of activated charcoal, graphite, and conventional charcoal carbonized in a static atmosphere. The resulting diffraction patterns indicated a high DOC in wood carbonized considering a static atmosphere. The change from disordered (or amorphous) to ordered (or crystalline) structure was apparent (Assis et al. 2016).

Results presented in Table 1 and Figure 3 shows that the more crystalline samples were eucalypt wood (16.1%), followed by sugarcane (14.9%), coconut (13.9%), and sisal (11.1%). Such results are in agreement with the cellulose/hemicellulose content from literature, as shown in Table 1. The most crystallized sample has the lowest expected cellulose/hemicellulose content (wood) and in opposition, sisal presented the lowest crystallized result – it is thus expected to present one of the highest cellulose/hemicellulose contents.

Thermal analysis

The main objective of this analysis was to study the behavior of these materials at different temperatures. TG is used to measure the mass loss either as a function of time (isothermal) or

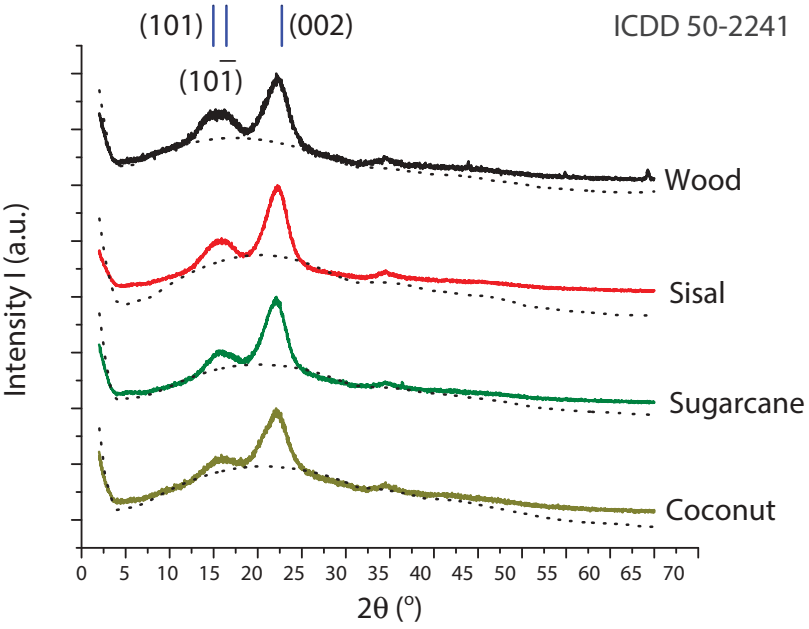

Figure 3. X-ray diffraction patterns of three plant fibers plus powdered wood over exposure angle range of 2–65° and respective Degrees of Crystallinity (DOCs), according to Equation (1): (a) coconut (13.9%); (b) sugarcane (14.9%); (c) sisal (11.1%); (d) eucalypt wood (16.1%). Dotted lines correspond to amorphous phase and the highest peak is indicated by plane (002). Experimental results are compared with ICDD 50–2241 card (cellulose I_β).

dynamic temperature and controlled atmosphere, and endothermic and exothermic changes in a DSC curve indicate events or reactions such as crystallization and melting. In the case of fibers and wood flour, endothermic peaks were observed, which are related to loss of components.

DTA is a highly used method in several areas of knowledge, where it is possible to obtain, besides the temperatures in which thermal phenomena occur and their nature (endothermic or exothermic), and the enthalpy variation brings transformations that occur as a function of temperature or time (Dweck 2015). From DTA analysis, the following graphs were constructed (Figure 4) under N_2 atmosphere. Figure 5 shows results under air. It is well known that sometimes is difficult to separate each event clearly, due to complex reactions that occur during the degradation process (Lomeli-Ramirez et al. 2014).

It is possible to note that the higher calculated DOC for wood matches the larger DTA crystallization peaks. It was also possible to assess that sugarcane had the highest dehydration percentage below 200°C, due to the higher endothermic peak at this temperature range. All samples also presented degradation around 300°C.

The four mass loss graphs have a similar behavior. Observing all, there are three main stages of mass loss. Considering the composition of the fibers (Yang et al. 2007), it is shown that the first mass loss range is related to the moisture of the sample. All fibers are not totally water free, and such content should then be related to this factor, or at least some interaction of the OH^- bonds with the fiber structure. These results are in agreement with the previous FTIR analysis. The second range, in the region between 220°C and 300°C, is related to the lignin degradation or its fractions, which are present in all fibers. This degradation is related to the degradation of ether and carbon–carbon bonds. The third range, from 300°C to approximately 450°C, refers to the decomposition of cellulose and hemicelluloses, which were observed by FTIR and X-ray results. From this temperature, a continuous peak tends to zero which is related to fiber degradation.

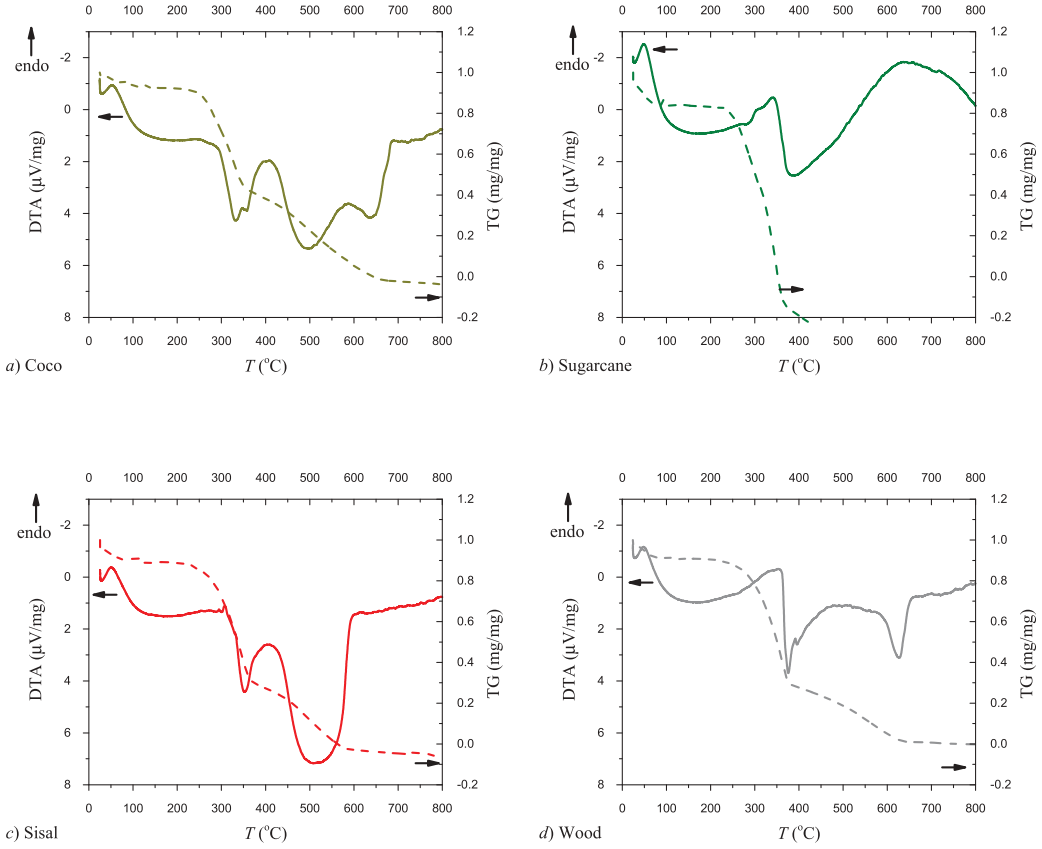

Figure 4. Thermogravimetric and DTA curves under nitrogen air at a heating rate of 10 K/min: (a) coconut; (b) sugarcane; (c) sisal; (d) wood.

According to Manfredi et al. (2006), vegetable fibers present degradation in two main stages. The first corresponds to hemicellulose thermal depolymerization and to the decomposition of the glycosidic bonds of the cellulose. The second is related to the decomposition of α-cellulose. Lignin decomposition occurs over a wide temperature range, between 200°C and 500°C (Manfredi et al. 2006). This can be observed in all fibers as well as wood flour, confirming IR data related to the composition of the materials.

However, these methods have limitations on the interpretations of the morphological and dimensional changes in the sample during analyses. In order to meet these limitations, a relatively new analysis procedure has been explored, which is heating microscopy (Dweck 2015), presented below.

Heating microscopy

Optical microscopy has been widely used by scientists and students as a useful tool to examine objects on a fine scale in order to get information relative to the morphology of the materials examined. Fibers and wood powder samples were inserted in a Linkam hot stage coupled to a Leica microscope with the same conditions applied for thermal analysis (and under air atmosphere).

The degradation of the fibers was not uniform, and this could be observed through the captured images. As the fibers are solid, the expansion was expected with heating. But this was not what happened. Instead, a percentage decreasing on diameter ($d(T)/d_0$) as well as length ($L(T)/L_0$) was observed, according to Figures 6 and 7. Such percentage changes are referred to their initial

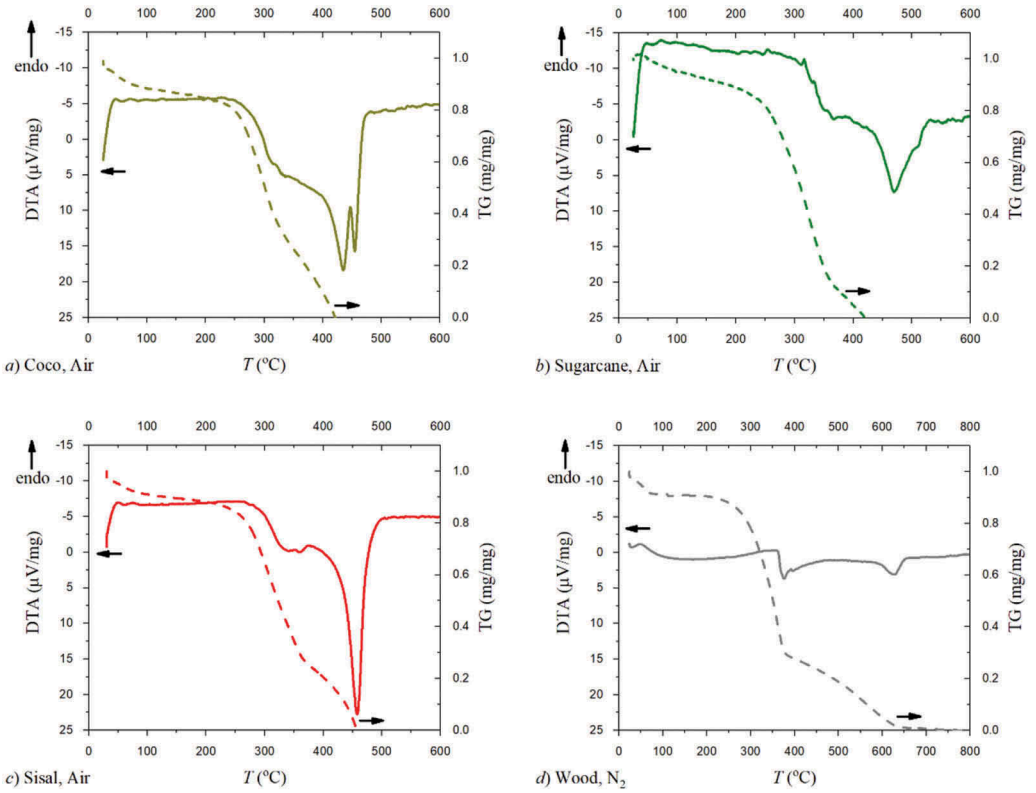

Figure 5. Thermogravimetric and DTA curves under air atmosphere at a heating rate of 10 K/min: (a) coconut; (b) sugarcane; (c) sisal; (d) wood.

respective dimensions (d_0 and L_0). In special, one particular event occurred: coconut, sugarcane, and sisal fibers were divided into two filaments at 200°C, and thus at these temperatures, there was a small increase in the diameters observed, as presented in Figure 6. It was observed that thickness decreased by 50% when heated at 450–500°C. This process started around 300–400°C with an initial percentage length of ≈ 90%, that corresponds to a fast weight loss. Such behavior is similar to results observed by Xu et al. (2017), that studied wood samples carbonized at temperatures from 200°C to 600°C, that became noticeable thinner during process observed by Scanning Thermal Microscopy, that used an atomic force microscope (XE-100, PSIA Corp., Sungnam, KO). In fact, they verified that thickness of wood cell walls decreased by 62% when samples were carbonized up to 600°C, and that such thickness loss occurred simultaneously with mass loss.

As far authors know, the first observation of the mass loss, density changes, and dimensional shrinkage of wood charcoal heat treated between 277°C and 400°C in the longitudinal, radial, and tangential directions are due to McGinnes, Kandeel, and Szopa (1971). They found reduced values of 25.68%, 15.45%, and 11.43%, respectively, taking into account measurements of microtomed cubes. Due to such different experimental procedures, these values are lower than the characteristics temperatures found in this work.

These events can be explained by the fact of the components present in the fibers, mainly hemicellulose and lignin, gives them certain elasticity, and with heating this characteristic is lost. It is observed that they begin to shrink and in some moments this shrinkage occurs rapidly, because at these temperatures the components at their elasticity limit, these points coincide with the loss of mass and are related precisely to the loss of cellulose and lignin. In fact, it is possible to observe a behavior when one compares data between thermogravimetry (or mass loss) and percentage length:

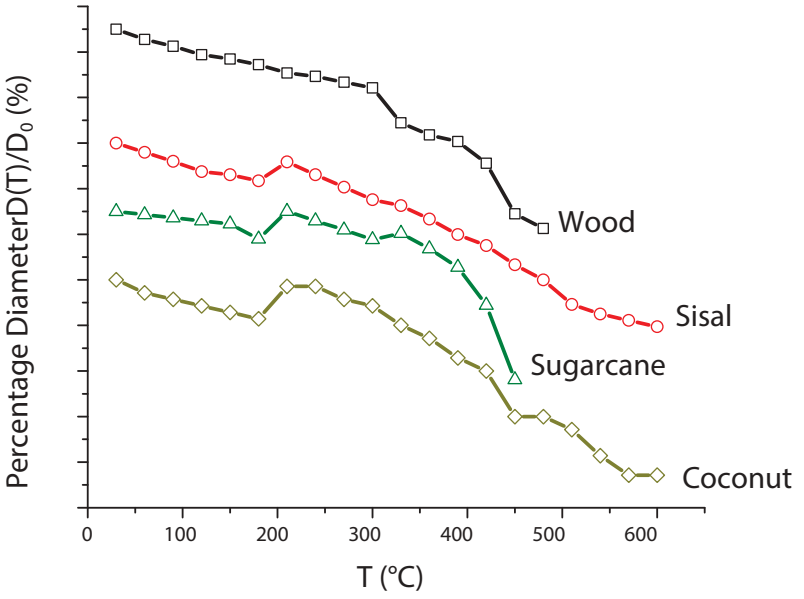

Figure 6. Variation of the percentage diameter of three fiber samples (coconut, sugarcane, and sisal) plus eucalyptus wood powder as a function of temperature up to 600°C. Such heating conditions were the same for TG/DTA analysis under air atmosphere.

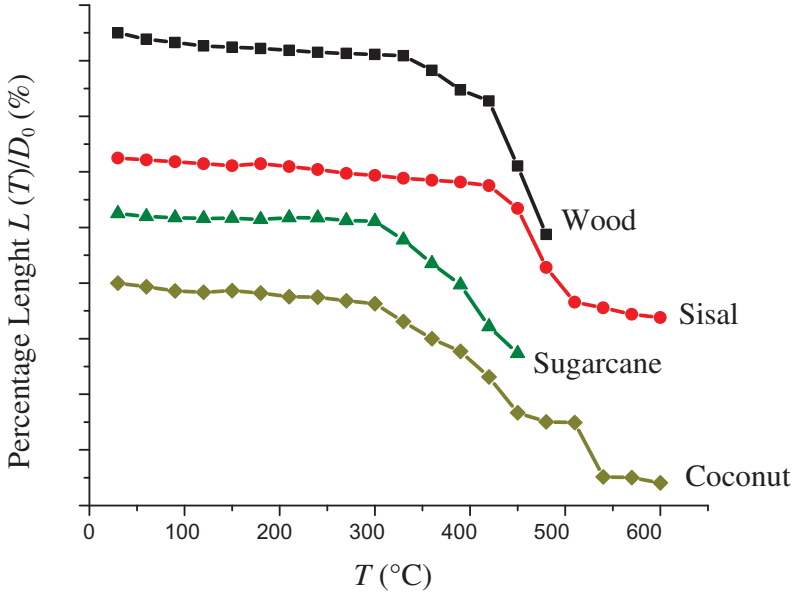

Figure 7. Variation of the percentage length of three fiber samples (coconut, sugarcane, and sisal) plus eucalyptus wood powder as a function of temperature up to 600°C. Such heating conditions were the same for TG/DTA analysis under air atmosphere.

the initial slow size decrease $L(T)/L_0$ is related to water loss. There is also an abrupt decreasing on $L(T)/L_0$ starting at 300°C for coconut and sugarcane; this change occurs at 350°C for eucalyptus wood and above 450°C for sisal, and are also related to mass loss observed in Figures 4 and 5.

As expected, at the beginning of heating process, water is released, promoting an endothermic effect as shown by DTA, according to Figures 4 and 5, but no morphological change was observed. As organics thermal decomposition begins around 200°C, as shown by respective TG curves in Figures 4 and 5, the endothermic effect follows continuously, promoting the formation of carbonaceous residues that begin to darken the captured images. As temperature increases, the higher was this effect, which at around 450°C turns image almost completely impossible to observe fibers, so that the analysis could not be followed visually until the end. However, the mass loss data lead to the conclusion that from this point a rapid degradation of the fiber occurs.

From heating microscopy technique, videos with sample images were obtained, at the same time as it was being heated at the same heating rate used for DTA and TG. Then, it was possible to present images with some characteristic temperatures, i.e., those that showed peaks in the heating curves (Figure 8) in order to better interpret the transformations occurring in all samples. All images correspond to thermal events presented in Figures 5–7.

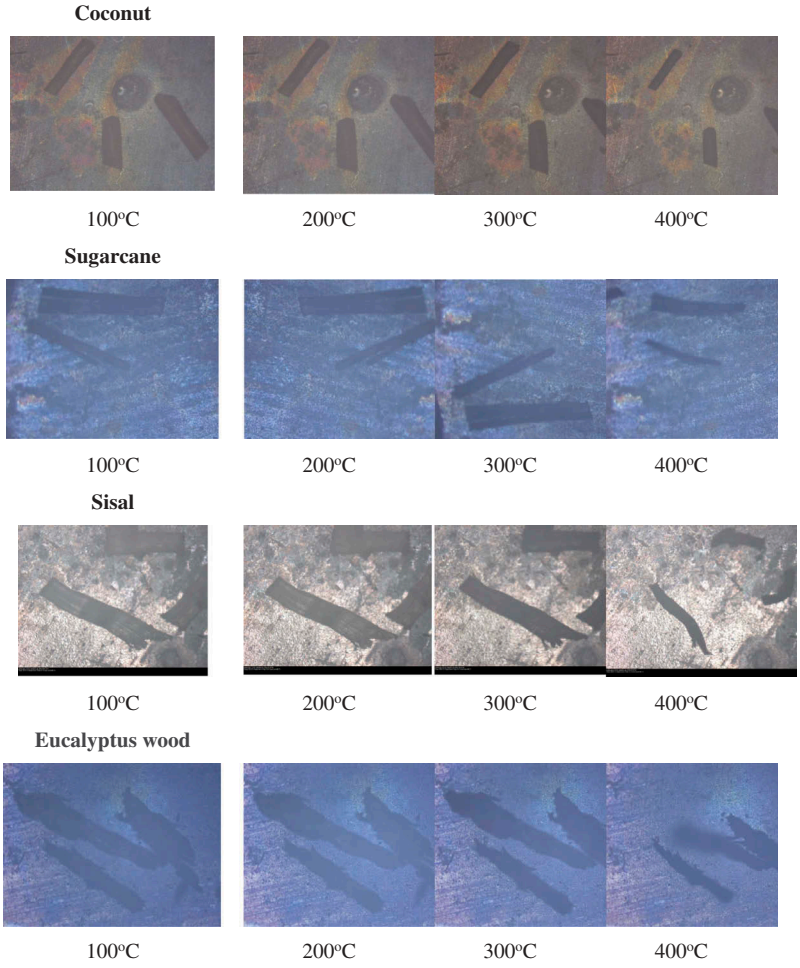

Figure 8. Images by heating microscopy of three fiber samples (coconut, sugarcane, and sisal) plus eucalyptus wood obtained at different temperatures (in °C), indicating specific shape or phase changes. Magnification 50×.

Conclusions

As expected, it was observed that FTIR spectra have the same behavior; all have absorption bands characteristics of the carbonyl, hydroxyl and C–OH groups. This leads to confirmation that all have in their structure near the same components. The variation in band lengths is related to the presence of groups in greater or lesser amounts of fiber components.

XRD results presented cellulosic structure and allowed calculating a DOC: sisal presented the lowest (11.1%) and eucalypt wood the highest amount (16.1%). Sugarcane and coconut presented almost the same amount (around 14%). Such results are in agreement with expected cellulose/hemicellulose contents presented in literature for each of those vegetable fibers.

The present study attempted to quantitatively analyze the shrinkage of vegetable fibers under heating. Dimensional shrinkage of fibers is not a simple process. Heating microscopy analysis is a good tool for measuring dimensional changes of samples submitted to heating process. During heating, the burning process of fiber components promoted the formation of carbonaceous residues that begin to darken the captured images. But it was possible to observe dramatic dimensional changes due to heat treatment.

The degradation of fibers was not uniform, and this could be observed through images and compared with traditional thermal analysis. As the fibers are solid (but almost amorphous), expansion with heating was expected. But this did not occur, because the components present in the fibers give them certain elasticity, mainly because of heating, this characteristic is lost. It was then observed that all fibers begin to shrink and that sometimes this shrinkage occurs rapidly. Most weight loss and shrinkage occurred before 300–400°C. These data coincide with the complete loss of the components of lignin and cellulose at near the same temperature interval observed by thermal analysis. This observed non-uniformity in the degradation can be related to the fact that the composition of the fibers varies considerably with the cellulose/hemicellulose composition, whose degradation is related to higher temperatures.

Funding

The authors thank the Brazilian CNPq agency for their financial support, in particular grant numbers 304705/2015-2 and 404004/2016-4.

ORCID

Luciano Pisanu http://orcid.org/0000-0001-7727-6978
Marcio Luis Ferreira Nascimento http://orcid.org/0000-0001-5030-7500

References

Assis, M. R., L. Brancheriau, A. Napoli, and P. F. Trugilho. 2016. Factors affecting the mechanics of carbonized wood: Literature review. *Wood Sciences and Technology* 50:519–36. doi:10.1007/s00226-016-0812-6.

Brahmakumar, M., C. Pavithran, and R. Pillai. 2005. Coconut fibre reinforced polyethylene composites: Effect of natural waxy surface layer of the fibre on fibre/matrix interfacial bonding and strength of composites. *Composites Science and Technology* 65:563–69. doi:10.1016/j.compscitech.2004.09.020.

Brigida, A. I. S., V. M. A. Calado, L. R. B. Gonçalves, and M. A. Z. Coelho. 2010. Effect of chemical treatments on properties of green coconut fiber. *Carbohydrate Polymers* 79:832–38. doi:10.1016/j.carbpol.2009.10.005.

Carvalho, L. F. M. 2004. Fibras de Palha de Carnaúba: Caracterização Térmica e Aplicação em Compósitos. Dissertação de Mestrado. Universidade Federal do Piauí (*in Portuguese*).

Dweck, J. 2015. Dimensional Thermal Analysis by Optical DSC. VII SiAT – Simpósio de Análise Térmica, Unesp - Bauru/SP 289-292.

Foelkel, C. E. B. 1977. *Quality of Wood*, 60. Viçosa: CENIBRA.(*in Portuguese*).

Herzog, R. O., and W. Jancke. 1920. Röntgenspektrographische Beobachtungen an Zellulose. *Zeitschrift Für Physik* 3:196–98. (*in German*). doi:10.1007/BF01331987.

Kisser, J. G., A. Ylinen, K. Freudenberg, F. F. P. Kollmann, W. Liese, B. Thunell, H. G. Winkelmann, W. A. Côté Jr., P. Koch, J. E. Marian, and A. J. Stamm. 1967. History of wood science. *Wood Sciences and Technology* 1:161–90. doi:10.1007/BF00350460.

Lomeli-Ramírez, M. G., S. G. Kestur, R. Manríquez-González, S. Iwakiri, G. B. Muniz, and T. S. Flores-Sahagun. 2014. Bio-composites of cassava starch-green coconut fiber: Part II – Structure and properties. *Carbohydrate Polymers* 102:576–83. doi:10.1016/j.carbpol.2013.11.020.

Lopes, W. A., and M. Fascio. 2004. Esquema para Interpretação de Espectros de Substâncias Orgânicas na Região do Infravermelho. *Química Nova*. 27:670–73. (*in Portuguese*). doi:10.1590/S0100-40422004000400025.

Madsen, I. C., N. V. Y. Scarlett, and A. Kern. 2011. Description and survey of methodologies for the determination of amorphous content via X-ray powder diffraction. *Zeitschrift Für Kristallographie* 226:944–55. doi:10.1524/zkri.2011.1437.

Manfredi, L. B., E. S. Rodríguez, M. Wladyka-Przybylak, and A. Vázquez. 2006. Thermal degradation and fire resistance of unsaturated polyester, modified acrylic resins and their composites with natural fibres. *Polymer Degradation and Stability* 91:255–61. doi:10.1016/j.polymdegradstab.2005.05.003.

McGinnes, E. A., S. A. Kandeel, and P. S. Szopa. 1971. Some structural changes observed in the transformation of wood into charcoal. *Wood Fiber* 3:77–83.

Medina, J. C. 1954. *O Sisal*. São Paulo: Secretaria de Agricultura do Estado de São Paulo. (*in Portuguese*).

Morandim-Giannetti, A. A., J. A. M. Agnelli, B. Z. Lanças, R. Magnabosco, S. A. Casarin, and S. H. P. Bettini. 2012. Lignin as additive in polypropylene/coir composites: Thermal, mechanical and morphological properties. *Carbohydrate Polymers* 87:2563–68. doi:10.1016/j.carbpol.2011.11.041.

Mwaikambo, L. Y., and M. P. Ansell. 2006. Mechanical properties of alkali treated plant fibers and their potential as reinforcement materials I. Hemp fibres. *Journal of Materials Science* 41:2483–96. doi:10.1007/s10853-006-5098-x.

Nägeli, C., and C. Cramer. 1858. *Pflanzenphysiologische Untersuchungen* ***2****, Die Stärkekörner*, 39. Zurich: Friedrich Schulthess. (*in German*).

Park, S., J. O. Baker, M. E. Himmel, P. A. Parilla, and D. K. Johnson. 2010. Cellulose crystallinity index: Measurement techniques and their impact on interpreting cellulose performance. *Biotechnology for Biofuels* 3:1–10. doi:10.1186/1754-6834-3-10.

Rietveld, H. M. 1969. A profile refinement method for nuclear and magnetic structures. *Journal of Applied Crystallography* 2:65–71. doi:10.1107/S0021889869006558.

Sanchez, E. M. S., C. S. Cavani, C. V. Leal, and C. G. Sanchez. 2010. Compósito de Resina de Poliéster Insaturado com Bagaço de Cana-de-Açúcar: Influência do Tratamento das Fibras nas Propriedades. *Polímeros* 20 (*in Portuguese*): 194–200. doi:10.1590/S0104-14282010005000034.

Sansigolo, C. A. 1994. Deslignificação em Metanol-Água de *Eucalyptus globulus*, Labill: características da lignina e da polpa. Tese (Doutorado em Ciências) – Instituto de Física e Química de São Carlos, Universidade de São Paulo, 163 (*in Portuguese*). doi:10.3168/jds.S0022-0302(94)77044-2

Satyanaryana, K. G., J. L. Guimarães, and F. Wypych. 2007. Studies on lignocellulosic fibers of Brasil. Part I: Source, production, morphology, properties and applications. *Composites Part A* 38:1694–709. doi:10.1016/j.compositesa.2007.02.006.

Schmidt, M. B. 1959. On the history, development, and application of the warm stage. *Journal of the Royal Microscopical Society* 79:119–24. doi:10.1111/jmi.1959.79.issue-2.

Segal, L., J. J. Creely, A. E. Martin Jr, and C. M. Conrad. 1962. An empirical method for estimating the degree of crystallinity of native cellulose using the X-ray diffractometer. *Textile Research Journal* 29:786–94. doi:10.1177/004051755902901003.

Sgriccia, N., M. C. Hawley, and M. Misra. 2008. Characterization of natural fiber surface and natural fiber composites. *Composites Particle A: Applied Science and Manufacturing* 39:1632–37. doi:10.1016/j.compositesa.2008.07.007.

Stricker, S. 1870. Introduction. In *Manual of human and comparative histology*, ed. S. Stricker, i–xxxvii. London: The New Sydenham Society.

Xu, D., T. Ding, Y. Li, Y. Zhang, D. Zhou, and S. Wang. 2017. Transition characteristics of a carbonized wood cell wall investigated by scanning thermal microscopy (SThM). *Wood Sciences and Technology* 51:831–43. doi:10.1007/s00226-017-0919-4.

Yang, H., R. Yan, H. Chen, D.-H. Lee, and C. Zheng. 2007. Characteristics of hemicellulose, cellulose and lignin pyrolysis. *Fuel* 86:1781–88. doi:10.1016/j.fuel.2006.12.013.